Available online at www.sciencedirect.com
SCIENCE DIRECT®
Journal of Nuclear Materials 321 (2003) 78–83
journal of nuclear materials
www.elsevier.com/locate/jnucmat

The response of a chromium doped alumina screen to keV and MeV ions

Kieran J. McCarthy [a,*], J. García López [b], F. Martín Hernández [a], Bernardo Zurro [a], A. Baciero [a], M.A. Respaldiza [b]

[a] Laboratorio Nacional de Fusión, Asociación Euratom-CIEMAT, Avenida Complutense 22, E-28040 Madrid, Spain
[b] Centro Nacional de Aceleradores, Parque Tecnológico 'Cartuja '93', Av. Thomas A. Edison, E-41092 Seville, Spain

Received 30 January 2003; accepted 31 March 2003

Abstract

We have characterised the response of a chromium-doped alumina screen '*Chromox*' to light ions (H^+ and He^+) accelerated to keV and MeV energies. In particular, we have determined the absolute luminosity in terms of the number of photons emitted per incident ion from the front and back faces of such a screen. This work has been motivated by the application of this material to a diagnostic for measuring fast ion losses, close to the plasma edge, from the hot plasmas in fusion devices, where its radiation hardness, compared to that of standard phosphors, makes it very attractive. We also discuss the persistent afterglow observed after removal of the ion beam in terms of its cause and possible repercussions for this diagnostic.

PACS: 81.05.J; 78.55.−m; 87.50.Gi; 61.80.Fe

1. Introduction

Several decades of research on ceramic phosphors at CERN and at other laboratories has led to the use of doped alumina ceramic screens, i.e. $Al_2O_3:Cr^{3+}$, [1–4] and Ce-doped YAG single crystal converters [5] for accelerator beam (electrons and ions) observations. In particular, such screens are compatible with ultrahigh vacuum systems, they exhibit good response linearity and are reported to exhibit good relative sensitivity to charged particles accelerated to MeV and GeV energies. Also, in tests made at CERN with doped alumina ceramic screens, they have withstood integrated relativistic proton fluxes of up to 10^{20} protons cm^{-2} [1], while tests made on polycrystalline Al_2O_3:Cr with He^+ ions accelerated to 200 keV showed a 50% decrease in radioluminescence for total doses above 10^{15} cm^{-2} [6]. In addition, in recent tests on a screen irradiated with electrons accelerated to 1.8 MeV, the luminescence output, when stimulated by extreme ultraviolet (EUV) radiation, fell to half its original level after a total dose of 2.5×10^{17} electrons cm^{-2} [7]. Such levels are a factor 10^3–10^4 higher than those for standard phosphors [8,9]. This property, as well as their immunity to electromagnetic interference and ground loops, and their compactness (only a thin screen is required), makes them particularly suited for use as broadband radiation detectors in the harsh environments encountered in fusion devices [10].

To date, diagnostics for detecting fast ion (H^+) losses from the hot plasmas of fusion devices, as well as fast alpha particle losses from D-T fusion devices [11], have employed thin phosphor screens, e.g. ZnS:Ag (P11) [12,13]. However, such phosphor screens cannot survive the harsh radiation environment encountered in a fusion device operated for long periods with deuterium and

* Corresponding author. Tel.: +34-91 3466372; fax: +34-91 3466124.
E-mail address: kieran.mccarthy@ciemat.es (K.J. McCarthy).

0022-3115/$ - see front matter © 2003 Elsevier B.V. All rights reserved.
doi:10.1016/S0022-3115(03)00208-3

tritium, moreover as the probe must be located close to the plasma outer edge. In contrast, we described recently two conceptual diagnostic systems [14], based on the collection of light induced by ions impacting on alumina ceramic screens for the TJ-II stellarator [15]. In the TJ-II device, future plasmas will receive up to 2 MW of additional heating from two neutral beam injector (NBI) systems in which neutral hydrogen is accelerated to 40 keV [16]. Moreover, theoretical studies predict that losses due to fast ions could reach 30% of the injected NBI power [14]. Therefore, in order to quantify the fast ion fluxes intercepted by such diagnostic systems, it is necessary to determine the absolute luminosity of Al_2O_3:Cr screens to high energy ions. In this paper, we describe measurements of the radioluminescence from a chromium-doped alumina ceramic screen (1 mm thick) irradiated with H^+ and He^+ ions having discrete energies between 50 keV and 1.75 MeV. We plot the results in terms of the number of photons emitted per incident ion and determine the efficiency (number of photons per MeV). Finally, we investigate its persistent afterglow, which is typical of luminescent ceramics, that is observed after the removal of the radiation.

2. Experimental set-up

The 46 mm diameter chrome-doped alumina screen under study, *Chromox-6*, was obtained from Morgan Matroc Ltd., East Molesey, England. The screen selected was 1 mm thick, it had a density of 3.96 $g\,cm^{-3}$, a grain size of 3–5 μm, and the alumina ceramic was doped with 0.5% chrome sesquioxide. The principal luminescence of Cr^{3+} in Al_2O_3 consists of two sharp lines (generally called the *R* lines), that arise from transitions from the lowest excited state (^2E) to the $^4A_2$ ground state of Cr^{3+}. At room temperature these lines occur at 692.9 and 694.3 nm and have a stated decay time of 3.4 ms [17]. It is also reported to exhibit good thermal stability, i.e. stable luminescence brightness (±15%), over the range from room temperature to 450 °C [1]. Although, additional strong lines may appear with increased Cr^{3+} concentrations, the *R* emission lines dominate for the 0.5% chrome sesquioxide samples and hence are the only emissions considered for analysis. See Fig. 1. Finally, self-absorption of the luminescent light efficiency in the screen can be approximated empirically as *Chromox-6* screens are translucent, having an attenuation coefficient $\alpha = 0.8 \pm 0.1\ mm^{-1}$ at 694 nm [1].

The measurements were made on the ion beam facility at the Centro Nacional de Aceleradores (Spanish National Accelerator Centre), Seville, Spain [18]. This facility is based around a 3 MV tandem accelerator (model 9SDH-2 by NEC). For these tests, H^+ ions were created in the SNICS II, a caesium-sputtering source with a TiH_2 cathode, while He^+ ions were generated by

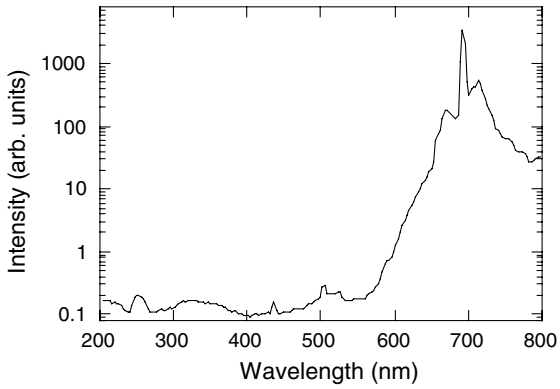

Fig. 1. The emission spectrum of chrome-doped alumina *Chromox-6*.

radio frequency within an Alphatross ion source. The resultant ions were then accelerated towards a 90° analysing magnet before passing directly to a general purpose IBA scattering chamber located at the end of beam line. The entrance to this chamber was equipped with collimation slits while an insulated chopper was positioned behind them to collect part of the ion beam current. The incident ion flux was determined by integrating this current for 120 s (to improve statistics) with a charge digitiser (OM35e) having a sensitivity of 10^{-12} C/pulse. See Fig. 2. Beam fluxes of the order 3×10^{11} $cm^{-2}\,s^{-1}$ for protons and 7×10^{12} $cm^{-2}\,s^{-1}$ for He^+ were employed. Finally, in order to degrade the ion energy, aluminised mylar® films (6 and 19 μm) were fixed to a vacuum indexible holder located inside the IBA chamber which could be translated into the beam when required. See Table 1 for incident and degraded ion energies.

The ceramic screen under investigation was placed in an in-house designed vacuum chamber consisting of a five-way vacuum cross (model CX5-63 by Caburn-MDC, England). This chamber was mounted directly onto the back end of the IBA chamber. The sample was held on the end of a combined rotary and linear motion feedthrough (model VF-180-3 by Huntington) that was mounted on a second way of the five-way cross [20]. This system permits measurements to be made at different positions across the sample (to reduce localised radiation damage) as well as at different screen/incident beam angles, i.e. with the ceramic set at 0° and 45° to the beam. Two photomultiplier tubes (PMTs) (model H5783-04 by Hamamatsu) located on the outside of in-house designed zero length viewports, that were mounted at the ends of the third and fourth ways, measured the light emitted from the sample. Note that the efficiency was measured in both reflection, i.e. the light emerging from the illuminated face of the screen, and transmission, i.e. the light emerging from the rear face of the screen. See Fig. 2. Next, apertures, located between

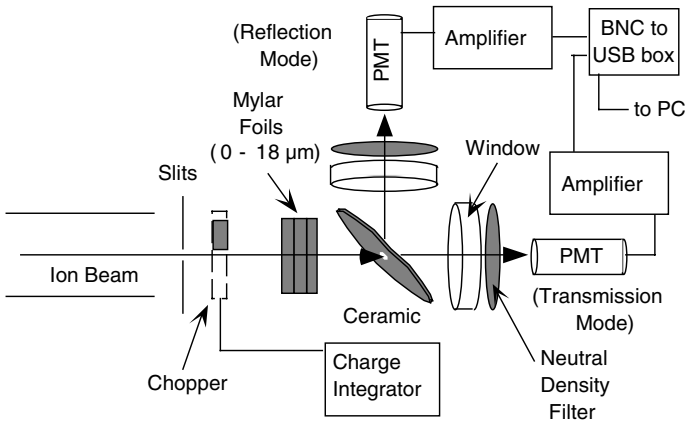

Fig. 2. A schematic diagram of the experimental set-up at CNA showing the ceramic and photo-multiplier detectors as well as the incident ion beam and light directions.

Table 1
The estimated mean energy of the He^+ ions and protons emerging from the rear of the mylar foils [19]

Ion	Incident ion energy (MeV)	Mylar foil thickness (μm)	Mean energy of emerging ions (keV)	Ion energy straggling (keV) FWHM
He^+	1.75	6	120	24
He^+	1.65	6	50	16
H^+	1.088	19	148	80
H^+	1.06	19	59.3	76.3

The full-width at half-maximum (FWHM) energy straggling of the emerging ions is also given.

the sample and detectors minimized reflections off the chamber walls. Also, because of the high output light levels from the samples, neutral density filters were placed in front of the PMTs. See Fig. 2. This was preferable to reducing the PMT sensitivity levels that would have resulted in reduced signal to noise levels. The signal currents from the PMTs were filtered and amplified by low noise current amplifiers (model SR570 by Stanford Research Systems, Sunnyvale, CA) before being fed via a BNC to USB converter box (Series 9800 by Data Translation Inc., Marlboro, MA) to a portable PC where the measured signals were logged and stored. Finally, light flashes were observed occasionally when measurements were being performed, these being more frequent for higher ion fluxes. See Fig. 3. We attribute these to the build up of charge in the irradiated part of the ceramic (it is a good electrical insulator). In order to avoid this a thin layer of conducting metal should be deposited on the screen and connected to ground [12]. Nonetheless, the light flashes were easily removed when processing the output signals. Finally, the luminescence decay behaviour of the ceramic was studied by *switching-off* the beam while recording the temporal evolution of luminescent signal. Once measurements were completed, the beam was blocked and background signal levels were recorded.

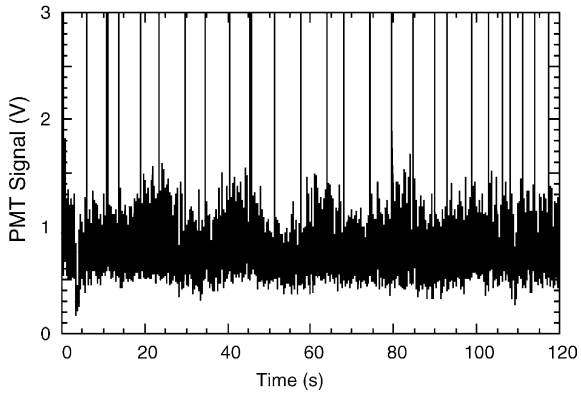

Fig. 3. The amplified output of the signal from the photo-multiplier set to view the rear side of the *Chromox-6* screen. The randomly occurring vertical lines are light flashes due to charge build-up on the ceramic.

3. Results and analysis

Several steps were required when post-processing the data. First, the ion beam flux incident on the ceramic was determined for each energy and particle type from the integrated pulse counter reading using the current digitiser sensitivity and known chopper correction

factors. At the energies under study here, the ions do not traverse the screen, rather they are stopped within the first 100 μm. Second, the fluxes of photons reaching the PMTs were determined from the time integrated light signals (see Fig. 3) using sensitivity curves provided by the manufacturer [21] while correcting for transmission losses in the vacuum windows, for light attenuation in the neutral density filters and for signal amplification. Note: the background signals were <0.1% of the light signals. Third, by taking account of the ceramic/PMT geometry, the number of photons emitted normal to the screen surface(s) per steradian was determined. As the screen to PMT separation was relatively small (~151.5 mm), the beam spot area (~16 mm^2) constituted an extended source. Hence the fractional solid angle to the detector was obtained using equations described in Tsoulfanidis for disk sources which result in a fixed error of ~1% for absolute measurements [22]. Finally, in Fig. 4, we plot, for the front and back of the screen, the number of visible photons emitted per steradian per incident ion for each particle type and energy. The measurements in this figure can be reproduced to within 5% with a relative uncertainty below 20%. The most significant sources of absolute uncertainty include the response of the H5783-04 PMT, ±10%, and the ion beam current, ±10%.

Charged particles such as protons or α particles lose energy through Coulomb interaction with electrons in a solid. For weakly penetrating particles of equal charge (low energy H^+ and He^+) the rate of energy loss increases as the mass of the particle increases, whereas the luminescence yield decreases [23]. For particles with equal energies, a He^+ ion will produce 0.2–0.4 times the light produced by H^+. Indeed, in these measurements this factor is 0.15–0.22, which is in good agreement with that above. Also, the radioluminescence of materials is generally described in terms of light yield. For this, many authors only consider the total light emitted from the rear face of the scintillation crystal under ion bombardment. Now, in order to make comparisons, it is necessary to consider the Lambertian fall-off in light intensity as a function of angle to the surface normal

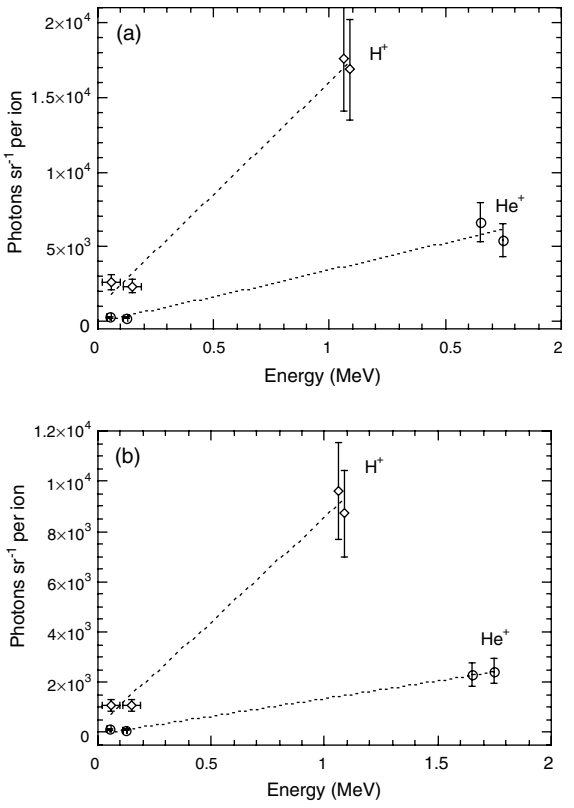

Fig. 4. Plots of the number of visible photons emitted per steradian from the Al_2O_3:Cr screen per incident H^+ and He^+ ion as a function of ion energy for emission normal to the screen surface in: (a) reflection and (b) transmission mode.

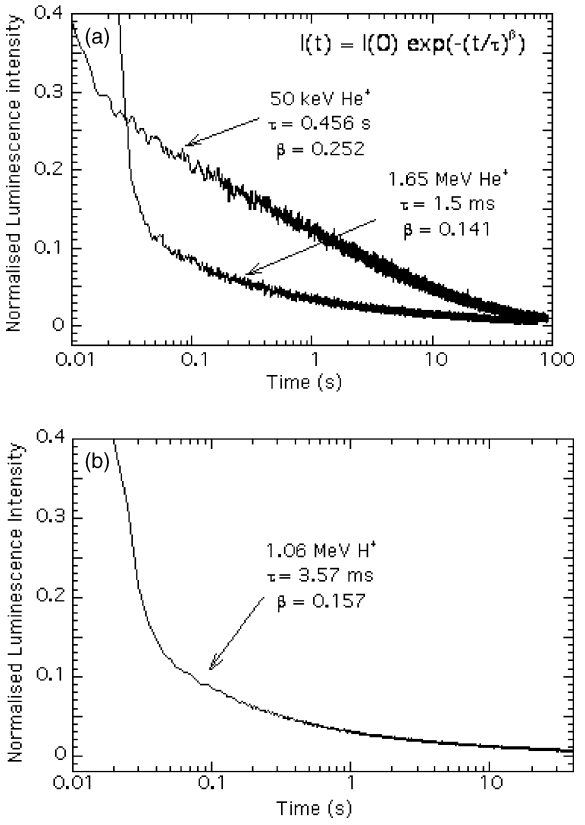

Fig. 5. The temporal evolution of the light emitted (normalized) from the ceramic after beam *switch-off* for: (a) He^+ and (b) H^+. The *Y*-axis has been expended to for clarity. The fitting parameters τ and β obtained from fitting the stretch exponential function [27] to the delayed luminescence are shown.

Table 2
Quantification of the persistent afterglow in the *Chromox-6* ceramic for H^+ and He^+ ions with different energies

Ion	1.06 MeV H^+	50 keV He^+	1.65 MeV He^+
Time to fall to 10%	~72 ms	1.9 s	~60 ms
Time to fall to 1% (s)	12	85	23
% Signal after 100 ms	8.6	20	8.4

The first and second rows show the times for the luminescence signal to fall to 10% and 1% of its values during irradiation while the bottom row indicates the percent signal at 100 ms after beam *switch-off*.

when estimating the total photon output. The resultant light yields, in terms of visible photons emitted from the *Chromox-6* screen are 4.35×10^3 and 1.105×10^4 ph/MeV for He^+ from the rear and front faces, respectively, and 2.68×10^4 and 4.94×10^4 ph/MeV for H^+. Indeed, the yield for He^+ of *Chromox-6* is comparable to that of the widely used scintillator YAP:Ce, i.e. 5.1×10^3 ph/MeV (after applying the quoted α/γ light yield ratio of 0.3 to the light yield for γ) [24,25].

The temporal evolution of the luminescence from the *Chromox-6* ceramic after the ion beam has been blocked, i.e. *switched-off*, for He^+ and H^+ is plotted in Fig. 5, while in Table 2, the times for the luminescence to fall to 10% and 1%, together with the percentage luminescence after 100 ms, are shown. In all cases a persistent afterglow, which decreases with increasing ion energy, is observed. Indeed, ceramic materials are known to show considerable afterglow after X-ray irradiation [26,27]. Indeed, the source of such afterglow has been investigated for a number of such materials. For instance, the afterglow from the ceramic $Gd_3Ga_5O_{12}$:Cr is explained by the fact that some of the electrons created by the X-rays are trapped by oxygen vacancies, whereas the holes are trapped by the Cr^{3+} ions [27]. The electrons recombine with these holes after thermal detrapping thereby yielding delayed luminescence. Also, in general, the afterglow curve is not represented by a simple exponential function, rather it is dependent on the concentration of such traps and on the electron capture cross-sections of the trap and the emitting centre [28]. For instance, the $1/t$ dependence in europium-doped alkali halides is explained by assuming a uniform distribution of trap depths [29]. Here, the decay can be fitted using the so-called Kohlrausch or stretched exponential function [30], see Fig. 5, where τ is effective lifetime and β is a dispersion parameter. Stretched exponential behaviour has been reported in the photoluminescence decay and transport properties of disordered systems such as amorphous semiconductors and glasses [31] and a model has been developed based on a random distribution of trapping centres [32]. Similar behaviour was observed when *Chromox-6* was irradiated with 2.5–4.5 keV X-ray radiation [26], with 20–50 keV X-rays [33], and with ions accelerated to MeV energies [34]. Finally, while a very short decay time may be imperative for many applications, it is not essential for our present application where we wish to determine the integrated ion flux entering our diagnostic. Moreover, in the testing phase for the proposed diagnostic, a radiation hard material is preferable as the conditions close to the hot plasma during the NBI phase are unknown at present.

4. Conclusions

The absolute luminosity of the chrome-doped alumina *Chromox-6* has been determined for low mass ions (H^+, He^+) accelerated to keV and MeV energies. The results obtained indicate that the signal levels from fast ion loss probes that employ this material as an incident ion to light transducer will not be signal limited, rather some attenuation may be required to avoid saturating the light detectors.

Acknowledgements

This work was partially funded by the Spanish 'Ministerio de Ciencia y Tecnología' (MCyT) under Grant No. FTN2000-0922. J.G.L. acknowledges the 'Ramón y Cajal' program of the MCyT for financial support.

References

[1] C.D. Johnson, The development and use of alumina ceramic fluorescent screens, European Laboratory for Particle Physics Report CERN/PS/90-42(AR).
[2] S. Yencho, D.R. Walz, IEEE Trans. Nucl. Sci. NS 32 (1985) 2009.
[3] S.D. Borovkov, S.A. Grishenkov, V.S. Konevskii, E.V. Krivonosov, L.A. Litvinov, V.P. Novikov, E.V. Serga, A.V. Kharlamov, Prib. Tekn. Eksper. 4 (1991) 33.
[4] T. Shirai, H. Dewa, Y. Iwashita, H. Okamoto, H. Fujita, S. Kakigi, A. Noda, M. Inoue, Bull. Inst. Chem. Res., Kyoto Univ. 71 (1993) 15.
[5] A.H. Lumpkin, B.X. Yang, W.J. Berg, M. White, J.W. Lewellen, S.V. Milton, Nucl. Instrum. and Meth. A 429 (1999) 336.
[6] N.T. My, Y. Aoki, H. Takeshita, S. Yamamoto, P. Goppelt-Langer, H. Naramoto, in: Y. Hama, Y. Katsumura, N. Kouchi, K. Makuuchi (Eds.), Proceedings of the

6th Japan–China Bilateral Symposium on Radiation Chemistry, Japan Atomic Energy Research Institute, Tokyo, 1995.
[7] K.J. McCarthy, A. Baciero, B. Zurro, U. Arp, C. Tarrio, T.B. Lucatorto, A. Moroño, P. Martín, E.R. Hodgson, J. Appl. Phys. 92 (2002) 6541.
[8] M.C. Ross, J.T. Seeman, R.K. Jobe, J.C. Sheppard, R.F. Stienin, IEEE Trans. Nucl. Sci. NS 32 (1985) 2003.
[9] W.A. Hollerman, J.H. Fisher, L.R. Holland, J.B. Czirr, IEEE Trans. Nucl. Sci. 40 (1993) 1355.
[10] A. Baciero, B. Zurro, K.J. McCarthy, P. Martín, M.C. de la Fuente, Rev. Sci. Instrum. 73 (2002) 283.
[11] S.J. Zweben, R.L. Boivin, C.-S. Chang, G.W. Hammett, H.E. Mynick, Nucl. Fusion 31 (1991) 2219.
[12] D.S. Darrow, A. Werner, A. Weller, Rev. Sci. Instrum. 72 (2001) 2936.
[13] M. Isobe, D.S. Darrow, T. Kondo, M. Sasao, K. Toi, M. Osakabe, H. Shimizu, Y. Yoshimura, C. Takahashi, S. Murakami, S. Okamura, K. Matsuoka, Rev. Sci. Instrum. 70 (1999) 827.
[14] C. Burgos, B. Zurro, J. Guasp, M.A. Ochando, K.J. McCarthy, F. Medina, A. Baciero, M. Liners, C. Fuentes, Rev. Sci. Instrum. 74 (2003) 1861.
[15] C. Alejaldre et al., Plasma Phys. Contr. Fusion 41 (1999) A539.
[16] J. Guasp et al., Fusion Technol. 35 (1999) 32.
[17] M. Tamatani, in: S. Shionoya, W.M. Yen (Eds.), Phosphor Handbook, CRC, Boca Raton, 1998.
[18] J. García López, F.J. Ager, M. Barbadillo Rank, F.J. Madrigal, M.A. Ontalba, M.A. Respaldiza, M.D. Ynsa, Nucl. Instrum. and Meth. B 161–163 (2000) 1137.
[19] P. Marmier, E. Sheldon, in: Physics of Nuclei and Particles, vol. 1, Academic Press, New York, London, 1969.
[20] A. Baciero, K.J. McCarthy, M.A. Acedo, L. Rodriguez-Barquero, J. Avila, Y. Huttel, V. Perez Dieste, M.C. Asensio, B. Zurro, J. Synchrotr. Rad. 7 (2000) 215.
[21] K.K. Hamamatsu Photonics, Photosensor Module H5783 Series, Technical data sheet (TPMHB0293EA), Shizuoka-ken, Japan, 1996.
[22] N. Tsoulfanidis, in: Measurement and Detection of Radiation, McGraw-Hill Series in Nuclear Engineering, Hemisphere Publishing Corporation, Washington, 1983.
[23] G. Blasse, B.C. Grabmaier, Luminescent Materials, Springer, Berlin, 1994.
[24] M. Moszynski, M. Kapusta, M. Mayhugh, D. Wolski, S.O. Flyckt, IEEE Trans. Nucl. Sci. 44 (1997) 1052.
[25] M. Moszynski, M. Kapusta, D. Wolski, W. Klamra, B. Cederwall, Nucl. Instrum. and Meth. A 404 (1998) 157.
[26] K.J. McCarthy, U. Arp, A. Baciero, B. Zurro, B.A. Karlin, J. Appl. Phys. (in press).
[27] G. Blasse, J. Alloys Compd. 225 (1995) 529.
[28] E. Nakazawa, in: S. Shionoya, W.M. Yen (Eds.), Phosphor Handbook, CRC, Boca Raton, 1998.
[29] I. Aguirre de Cárcer, F. Cussó, F. Jaque, Phys. Rev. B 38 (1988) 10812.
[30] R. Kohlrausch, Ann. Phys. (Leipzig) 12 (1847) 393.
[31] L. Pavesi, M. Ceschini, Phys. Rev. B 48 (1993) 17625.
[32] D.L. Huber, Phys. Rev. B 31 (1985) 6070.
[33] A. Ibarra, CIEMAT, Madrid, private communication.
[34] A. Peters, H. Eickhoff, T. Haberer, A. Weiss, Proceedings 8th European Particle Accelerator Conference, La Vilette, Paris, France, 2002, p. 1960.